Contents lists available at Science-Gate

International Journal of Advanced and Applied Sciences

Journal homepage: http://www.science-gate.com/IJAAS.html

Effects of Gum Arabic and its nanoparticles on hepato-renal toxicity induced by bromobenzene in male rats: Physiological, histological, and immunological studies

Turki M. Al-Shaikh [1, 2, *]

[1]Department of Biological Sciences, Faculty of Science, Northern Border University, Arar, Saudi Arabia
[2]Department of Biology, College of Science and Arts at Khulis, University of Jeddah, Jeddah, Saudi Arabia

ARTICLE INFO

Article history:
Received 24 May 2022
Received in revised form
24 October 2022
Accepted 6 November 2022

Keywords:
Antioxidant
Bromobenzene
Caspase-3
Gum Arabic
Kidney
Liver
Nanoparticles

ABSTRACT

This experimental study investigates the possible protective effects of Gum Arabic (GA) and its nanoparticles in hepato- and reno-toxicity induced by bromobenzene (BB) in rats and possible mechanisms of action. Thirty-five adult male albino rats were sorted into the following: Group 1 (control), Group 2 (NPs), Group 3 (GA, received 2 ml/kg of 10%w/v aqueous suspension), Group 4 (Gum-NPs, received GA loaded NPs), Group 5 (BB), received 460 mg/kg, Group 6 (GA+BB) and Group 7 (GA-NPs+BB). Treatment was via oral gavage daily for 10 days. Liver and kidney functions were measured in sera and total antioxidant capacity (TAC) was measured in tissue homogenates, and renal and hepatic tissues expression of caspase-3 were immuno-histochemical assessed beside histological alteration using a light microscope. BB treatment produced impairment of liver and kidney functions and decreased TAC activities and increased caspase-3 expressions in the liver and kidney and altered liver and kidney structures. Co-administration of GA and GA loaded on NPs for 10 days alleviated damaged effects of BB, especially in GA-NPs groups in liver and kidney functions and structures, and decrease expression of caspase-3 in the tissues. In conclusion, GA and its NPs had protective actions versus BB-induced destruction of the kidney and liver due to its antioxidant, anti-inflammatory and anti-apoptosis actions.

1. Introduction

Bromobenzene (C6H5Br) is a factory solvent utilized in the production of various chemicals and pharmaceuticals, as a flame retardant, crystallizing agent, and motor oil addition. Humans are exposed to bromobenzene (BB) during its manufacturing or utilization in different sectors, as well as through motor oil contamination. Because it is a hydrophobic chemical, BB bio-transformed in the liver and its metabolites are generated. The kidneys were exposed to 2, 3-epoxy BB, and 2-bromohydroquinone, that converted to 2-bromoquinone (Pannala et al., 2020). BB delivery at high doses led to a decrease in glutathione (GSH) levels due to conjugation to these metabolites, and therefore intracellular defense versus reactive oxygen species (ROS) was missed (Park et al., 2005). Secondary events that harm cells include lipid peroxidation, ATP deficiency, mitochondrial malfunction, energy disturbance, and alterations in intracellular calcium values (Akkara and Sabina, 2020).

Gum Arabic (GA) get from the exudates of Acacia Seyal or Acacia Senegal plants. GA is made from polysaccharides (the main component), oligosaccharides, and glycoproteins, as well as high levels of potassium, calcium, and magnesium ions (Isobe et al., 2020); however, its compositions differ according to its soil, climate, and source. Sudan is the world's most producer, then various countries in Africa (Isobe et al., 2020). GA dissolves in water to generate gel solutions with low viscosity. It is employed as a thickening substance, emulsifier, and enhanced stabilizer in the pharmaceutical and food sectors, as well as in the textile, ceramics, and cosmetics factories (Williams and Phillips, 2021). The Joint FAO/WHO Expert Committee on Food Additives evaluated GA for man's recommended daily intake (WHO, 1974). It is indigestible to both

* Corresponding Author.
Email Address: turkialshaikh808@gmail.com
https://doi.org/10.21833/ijaas.2023.02.019
Corresponding author's ORCID profile:
https://orcid.org/0000-0002-4469-8581

humans and animals, is not degraded in the intestine, but ferments in the colon to form short-chain fatty acids, leading to numerous health benefits (Calame et al., 2008). One of these benefits is its prebiotic action (Calame et al., 2008). Four weeks of GA (10 g/day) supplementation resulted in considerable increases in Bifidobacteria, Lactobacteria, and Bacteroides, indicating a prebiotic activity (Calame et al., 2008). Other actions are a decrease in plasma cholesterol value in animals and humans, anticarcinogenic action (Nasir et al., 2010), anti-inflammatory and anti-oxidant action with a protective effect versus liver and heart toxicities (Ali et al., 2011; Al-Kenanny et al., 2012). Also, GA is used as a pain reliever, offsets diarrhea, is anti-microbial, enhances teeth re-mineralization, and improves kidney functions in chronic renal failure (CRF) patients (Nasir et al., 2010). Few previous research has looked at GA's ability to reduce medication and chemical-induced toxicity (Ayaz et al., 2017).

Because tiny size materials have distinct qualities and features from those at larger scales, nanotechnology, defined as the technology in which materials and structures are present at nanometric scales, has elevated its application and research. Due to their multifunctional properties, magnetic nanoparticles (MNPs) have a lot of interest as a) Magnetic resonance imaging (MRI) can benefit from inherent magnetization features (Xie et al., 2011), b) non-invasiveness due to their magnetic targeting potential (Laurent et al., 2014), and c) its ability to operate as a biocompatible medication delivery system (Bashir and Haripriya, 2016).

The goal of this experimental research was to judge the protective actions of an aqueous extract of GA and its NPs against BB-induced hepato-renal toxicity in adult male rats. The examination was carried out by assessing numerous hepatic and kidney functions in the serum, as well as total antioxidant capacity (TAC) in tissue homogenates. Liver and kidney histopathological findings and immuno expression of apoptotic marker caspase-3 in hepatic and renal tissue were also evaluated.

2. Material and methods

2.1. Chemicals

GA got from a local market in Jeddah, Saudi Arabia, and used in aqueous extract formation. The dried gum is crushed into a fine powder and stored in airtight plastic containers at 5°C till used. Gum extract (10% w/v) is prepared by soaking 10 grams of gum in 100 ml of distilled water for 24 hours, then filtering it. The extract was newly formed daily (Zhang et al., 2009). BB got from Sigma Chemical Co. (St. Louis, MO, USA).

2.2. Preparation of magnetic nanoparticles

Ferrous chloride and ferric chloride 10 mM were added to 1.5 M of sodium hydroxide solution under stirring at a temperature of 75°C. The mixture was stirred with nitrogen gas protection for one hour. MNP was separated by using a magnetic separator and then washed with distilled water for five times (Zhang et al., 2009).

2.3. Preparation of GA magnetic nanoparticles (GA-MNP)

One ml of previously prepared MNP with a concentration of 10 mg/ml was added to 5 ml of 10% GA, and the mixture vortexed for 1 min followed by sonicated for 10 min. The GA-MNP was separated by a magnetic separator and washed five times with distilled water (Zhang et al., 2009).

2.4. Characterization of the GA

2.4.1. Entrapment efficiency measurement

The dialysis tubing technique was used to purify synthesized nano-formulations. GA is used to remove contaminants and liberate non-conjugated compounds from a solution by eluting it via regenerated cellulose (Amicon 10,000 MWCO ultrafilter, Millipore, USA). GA's entrapment efficiency (EE percent) was tested and processed using a microplate reader (BMG Labtech, Germany). The efficiency of compound entrapment was calculated by dividing the amount of compound incorporated into the NPs by the total amount of compound provided.

2.4.2. Transmission electron microscopy (TEM)

Transmission electron microscopy was utilized to analyze the particle morphology of GA (TEM, Philips CM-10, FEI Inc., Hillsboro, OR, USA). 100 g/mL of nano-suspension was put into formvar-coated copper grids, and samples were stained with two percent w/v uranyl acetate after complete drying (Electron Microscopy Services, Ft. Washington, PA). Digital Micrograph and Soft Imaging Viewer Software were used to capture and analyze images.

2.4.3. Zeta potential analyses

Photon correlation spectroscopy (PCS) was utilized to assess the zeta potential of NPs using a Zeta Sizer (Nano ZS, Malvern Instruments, UK). Samples were kept at a temperature of 25.0°C.

2.5. Animals

Thirty-five adult male albino rats (10-13 weeks) were used. Male rats only were chosen in this study as females had a circadian variation of hormones in the estrus cycle and that might alter levels of measured parameters. Rats were getting from the animal house at King Fahd Medical Research Center, Jeddah, Saudi Arabia. Animals were sorted in separate cages (n=5) and observed for one week for

acclimatization to a laboratory environment at a controlled temperature (22–24°C) with a normal light-dark cycle and relative humidity of 60-70%. Animals were enabled for free to get ordinal rats' diet and tap water. Experiments were made according to the Ethical Guidelines of Animal Care and Use Committee of King Abdelaziz University (KAU), Protocol Number 300-19.

2.6. Experimental design

Following acclimatization, animals were randomly sorted equally into seven groups. The experiments continued for 10 days were sufficient duration to elicit changes in liver and kidney tissues and animals received treatment via oral gavage daily for 10 days as follows:

- Group 1 (control group): Rats administered 1 ml/kg olive oil (vehicle of BB),
- Group 2 (NPs group): Rats received blank nanoparticles,
- Group 3 (GA group): Rats received an aqueous suspension of GA powder (2 ml/kg of a 10%w/v aqueous suspension) (Ali et al., 2003),
- Group 4 (GA-NPs group): Rats received GA-loaded NPs,
- Group 5 (BB group): Rats received BB (460 mg/kg in 1 ml olive oil) (El-Sharaky et al., 2009),
- Group 6 (GA+BB group): Rats received BB+GA as groups 3 and 5, and
- Group 7 (GA-NPs+BB group): Rats received BB+GA loaded nanoparticles as groups 4 and 5.

2.7. Biochemical parameters

At the experimental end, non-fasting blood samples (3 ml) were collected from each rat through the retro-orbital vein of the eye into plain tubes. Blood samples were left for 10 minutes and then centrifuged for 10 minutes at 4,000 rpm to get sera that were kept at −20°C till analysis. Sera utilized to determine liver function tests [aspartate amino transaminase (AST), alkaline phosphatase-(ALP), alanine amino transaminase (ALT), gamma-glutamyl transferase (GGT), total bilirubin (TB), total proteins (TP) and albumin] and kidney function tests [serum levels of creatinine, urea, and uric acid] according to manufacturer instructions. Following blood collection, samples of liver and kidney tissues (between 0.05 and 0.1 grams) were homogenized in phosphate buffer (0.1 M, pH 7.4) to provide a 20% w/v homogenate (Hitachi model EBA 12R, Germany).

This homogenate was centrifuged at 3000 g for 10 minutes at 4°C, and the supernatant was kept at -20°C till analysis. The homogenates were used for estimation of total antioxidant capacity (TAC) levels using Quantitative Sandwich ELISA kits for rats [My BioSource Company, *via* Mansour Scientific Foundation for Research and Development Company (MSFRDC), SA] according to manufacturer instructions.

2.8. Histological examination

Formalin (10%) was used to fix liver and kidney tissues that were then treated with graded ethanol and xylene. To prevent air entry, the tissues were placed in paraffin blocks. Using a rotary microtome machine, paraffin blocks were sliced into slices of roughly 5 m thickness. Following slicing, tissues were placed on glass slides and stained with hematoxylin and eosin (H&E) based on standard procedures. A light microscope was used to view stained tissue sections and photograph them. The leftover tissues were kept at -80°C until they were used in molecular research.

2.9. Immunohistochemistry study

The kidney and liver-positive slides were transferred to 10 mM sodium citrate buffer. Endogenous peroxidase blocked hydrogen peroxide, followed by anti-caspase-in blocking solution added to liver and kidney tissues, respectively.

2.10. Data analysis

Data expressed as mean+/-standard deviation and analyzed by IBM SPSS Statistics for Windows, version 23 (IBM SPSS, IBM Corp., Armonk, N.Y., USA). Shapiro–Wilk test was utilized to evaluate the normal distribution of data. One Way ANOVA test followed by Mann Whitney test for abnormally distributed values and least significant difference (LSD) for normally distributed data were used to compare results between various studied groups. *P*-values <0.05 are considered statistically significant.

3. Results and discussion

3.1. Characterization of modified GA with magnetite and chitosan nanoparticles

3.1.1. Magnetic GA nanocomposites

High-resolution transmission electron microscopy (HR-TEM) showed that the average size of magnetic GA nanocomposites ranged from 9.17 to 13.22 nm (Fig. 1A). Selected area electron diffraction (SAED) pattern demonstrated that the highly crystalline structure of magnetic GA nanocomposites (Fig. 1B).

3.2. Fourier-transform infrared spectroscopy (FTIR)

FTIR spectra for GA and magnetic GA linked with chitosan nanoparticles were shown in Fig. 2. The peak corresponding to C-H vibration at 2982 cm^{-1} was decreased after being linked with magnetite and chitosan nanoparticles. Also, the peak at 1620 cm^{-1} which corresponds to the carboxylate group was decreased due to the interaction of $-NH_2$ group with $-COO^-$ group. A strong peak appeared at 1085 cm^{-1}

which is related to C-O stretching and was decreased after modification with magnetite and chitosan nanoparticles (Fig. 2).

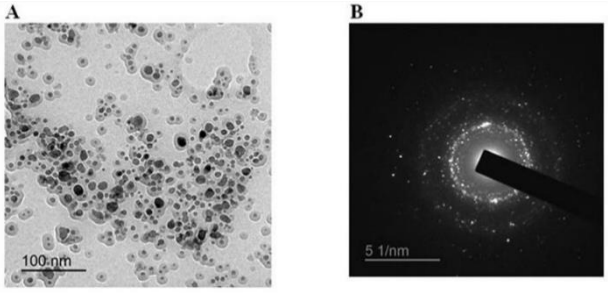

Fig. 1: Magnetic GA nanocomposites. A: High-resolution transmission electron microscopy (HR-TEM); B: Selected area electron diffraction (SAED)

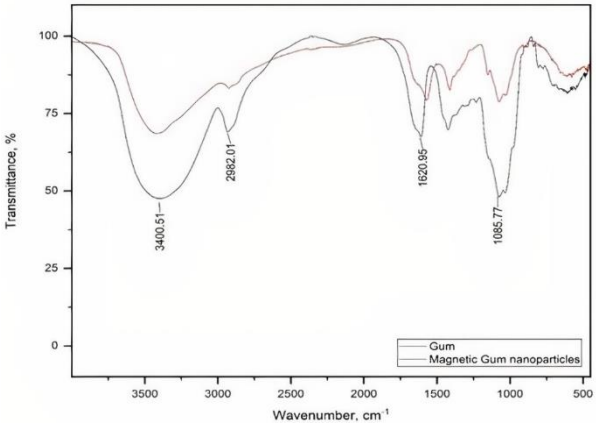

Fig. 2: Fourier-transform infrared spectroscopy (FTIR) of magnetic GA nanocomposites and GA

3.3. Zeta potential

Zeta potential analysis of GA functionalized with magnetite coated with chitosan nanoparticles was +48.5 mV.

In the present study, nano-formulation of GA was tested for its ability to ameliorate BB reno-hepatic toxicity in rats. The formulation of substances from elemental or herbal sources as nano-particles with scales ranging from 1-100 nanometers was reported to have unique characteristics and functions that change greatly from those seen at the bulk scale. This formulation enhanced solubility and multifunctionality, allowing it to target and treat a variety of disorders as well as mitigate toxic assaults (McNeil, 2005). Unique drug delivery systems used nano-formulation in the medicinal field and proved to be effective (Emerich and Thanos, 2003). Gum acacia was used to stabilize sliver nanoparticle formulation and to enhance biological activity (Rao et al., 2018).

3.4. Biochemical studies for liver and kidney function tests

Table 1 shows liver function tests in different studied groups. There was a significant elevation in serum values of ALT, AST, ALP, GGT, and TB but a significant decline in albumin and TP in BB and GA+BB groups versus control, NPs, and GA groups (P<0.050). Also, there were significantly elevated serum values of GGT and TB but a significant decrease in albumin in the GA-NPs+BB group versus control, NPs, and GA groups (P<0.050). Meanwhile, ALT in the GA-NPs+BB group versus was significantly elevated versus control, NPs; AST was significantly increased versus NPs.

Table 2 shows kidney function tests in different studied groups. There was a significant elevation in serum values of urea and creatinine in BB and GA+BB groups versus control, NPs, and GA groups (P<0.050) and in uric acid in GA-NPs+BB groups versus control and NPs (P<0.050).

Table 1: Comparison of serum levels of liver function tests in various studies groups

Variables	Control	NPs	GA	GA-NPs	BB	GA +BB	GA-NPs+ BB
ALT (U/L)	55.40±3.91	58.00±2.38	59.14±3.44	58.83±2.79	136.29±7.27^{a,b,c}	74.86±3.48^{a,b,c}	63.43±4.35^{a,b}
AST (U/L)	215.20±19.94	209.29±6.26	214.71±9.32	217.50±9.35	325.00±10.80^{a,b,c}	261.57±8.89^{a,b,c}	228.14±17.08^{b}
ALP (U/L)	65.60±4.67	67.43±3.41	69.43±3.26	70.83±2.04	98.57±9.43^{a,b,c}	83.00±2.70^{a,b,c}	65.43±7.25
GGT (U/L)	5.60±1.14	6.00±1.15	6.00±0.82	6.00±0.89	17.00±1.53^{a,b,c}	14.29±2.21^{a,b,c}	12.43±1.72^{a,b,c}
Total Bilirubin (TB)(mg/dL)	0.25±0.01	0.27±0.02	0.27±0.02	0.28±0.02	0.50±0.03^{a,b,c}	0.41±0.03^{a,b,c}	0.34±0.02^{a,b,c}
Total protein (TP)(g/dl)	5.10±0.48	4.97±0.32	4.90±0.26	5.00±0.28	3.29±0.25^{a,b,c}	3.89±0.31^{a,b,c}	4.55±0.55
Albumin (mg/dL)	2.78±0.13	2.90±0.08	2.84±0.13	2.85±0.10	1.46±0.17^{a,b,c}	2.21±0.20^{a,b,c}	2.54±0.11^{a,b,c}

ATL: Alanine aminotransferase; AST: Aspartate aminotransferase; ALP: Alkaline phosphatase; GGT: Gamma-glutamyl transferase. a: Significance versus control; b: Significance versus nanoparticles; c: Significant versus GA. Significance was made by Mann Whitney test as data were abnormally distributed

Table 2: Comparisons of kidney function tests in various group

Variables	Control	NPs	GA	GA-NPs	BB	GA +BB	GA-NPs+ BB
Serum creatinine (mg/dL)	0.11±0.01	0.12±0.01	0.12±0.01	0.13±0.01	0.62±0.05^{a,b,c}	0.30±0.04^{a,b,c}	0.21±0.02^{a,b,c}
Serum urea (mg/dL)	46.20±1.79	46.00±2.16	46.14±1.07	44.50±1.87	80.00±2.77^{a,b,c}	72.29±2.43^{a,b,c}	61.00±2.94^{a,b,c}
Serum uric acid (mmol/L)	0.55±0.03	0.56±0.03	0.59±0.03	0.56±0.01	1.67±0.20^{a,b,c}	0.84±0.05^{a,b,c}	0.62±0.02

a: Significance versus control; b: Significance versus nanoparticles; c: Significant versus GA. a: Significance versus control; b: Significance versus nanoparticles; c: Significant versus GA. Significance was made by Mann Whitney test as data were abnormally distributed

3.5. The antioxidant status of total antioxidants capacity in liver and kidney homogenates

Table 3 shows the total antioxidant capacity in liver and kidney homogenates in different studied groups. There was a significant decrease in hepatic and renal homogenate levels of TAC in BB, GA+BB, and GA-NPs+BB groups versus control, NPs, and GA groups (P<0.050).

Table 3: Comparison of total antioxidant capacity in liver and kidney homogenates in different studied groups

Variables	Control	NPs	GA	GA-NPs	BB	GA +BB	GA-NPs+ BB
Liver TAC (mM/gram proteins)	0.26±0.03	0.27±0.02	0.26±0.03	0.25±0.02	0.11±0.03 [a,b,c]	0.17±0.02 [a,b,c]	0.22±0.03 [a,b,c]
Kidney TAC (mM/gram proteins)	0.54±0.03	0.53±0.01	0.54±0.02	0.56±0.03	0.26±0.03 [a,b,c]	0.40±0.02 [a,b,c]	0.48±0.11 [a,b,c]

BB: Bromobenzene; GA-NPs: GA nanoparticles, TAC: Total antioxidant capacity. a: Significance versus control; b: Significance versus nanoparticles; c: Significant versus GA. Significance was made by Mann Whitney test as data were abnormally distributed

3.6. Histopathological assessments

3.6.1. Histological assessment of the liver

3.6.1.1. Hematoxylin and eosin stain

Fig. 3 reveals histological structure changes in the liver in different studied groups. The liver of control normal rats (G1) showed that lobular architecture was not well defined and marked only by central veins (CV) location. Hepatocytes were polyhedral in shape, having homogenous slightly basophilic cytoplasm and active vesicular one or two nuclei. Blood sinusoids separating hepatic cords were thin and showed flat nuclei. G2 (NPs) showed no alteration in the CV region. Hepatocytes looked normal or more organized compared to the control with vesicular active nuclei. G3 (GA) and G4 (GA-NPs) showed no apparent changes, except for a few scattered cells showing unstained cytoplasm. Most hepatocytes in the CV region showed homogenously stained cytoplasm and active vesicular nuclei. In G5, hepatocytes showed marked disorganization of cell cords. Some hepatocytes showed necrosis, shrinkage, and clumping and others showed vacuolation. Hepatic sinusoids could not be identified among necrosis cells. In G6 (GA+BB), the liver showed an absence of degenerative changes observed in G5 (BB group) with preservation of hepatocytes' normal structure and intervening sinusoids. G7 (GA-NPs+BB) showed more preservation of normal hepatocytes and sinusoid architecture. Hepatocyte nuclei were larger and more euchromatic indicating cell activity.

3.6.1.2. Immunohistochemical assessment of Caspase-3 expression in hepatic tissues

Immunohistochemical staining of caspase-3 (apoptosis marker) in rat liver of different groups was shown in Fig. 4. Mild reactions in blood sinusoid walls were observed in the liver of G1 (control). G2 (NPs), G3 (GA), and G4 (GA-NPs) caspase-3 immunostaining was similar to the control group. Meanwhile, G5 (BB group) revealed marked positive immunostaining of caspase-3 in degenerated (apoptotic) hepatocytes described in H&E slides. A decrease in caspase-3 immunostaining to be similar to control was observed in G6 (GA+BB) with better improvement in G7 (GA-NPs+BB). Hepatocytes of G6 and G7 possessed active large nuclei.

3.6.2. Histological assessment of kidneys

3.6.2.1. Hematoxylin and eosin stain

Fig. 5 reveals the renal histological changes in different studied groups. In control normal rats (G1) kidney tissue could be differentiated into an outer cortex and inner medulla. Renal corpuscles were well organized in the outer cortex consisting of clusters of collapsed capillaries within the Bowman capsule.

Normal glomeruli looked highly cellular due to endothelial cells nuclei and those of podocytes of the visceral layer of the Bowman capsule. The outer layer of the Bowman capsule was lined by a single layer of squamous cells. Around corpuscles, renal tubules cut in cross or oblique sections could be observed. The most dominating tubules were proximal ones with narrow lumina and cuboidal cells. Distal tubules had wider lumina and low cuboidal cells. Around the tubules, thin-walled collapsed capillaries could be seen. The upper medulla showed proximal, distal, and collecting tubules. In G2 (NPs), G3 (GA), and G4 (GA-NPs) kidneys' parenchyma looked similar to the control without an apparent histological alteration in renal corpuscles or renal tubules. Administration of BB to rats resulted in marked histological changes in kidney parenchyma as seen in G5. Vascular congestions of both glomerular and peritubular capillaries were observed. Marked degeneration of tubular epithelium where cells looked unstained with loss of apical brush border, smaller dark pyknotic nuclei were seen among renal corpuscles. Luminal casts could be seen in some tubules. Renal corpuscles also showed decreased glomerular cellularity and fibrosis (lobulated shrunken glomerular capillaries). Some samples showed inflammatory cells around necrosed tubules. In G6 (GA+BB), some renal corpuscles and tubules were normal compared to control, few showed dilation and luminal deposits in tubules. In G7 (GA-NPs+BB) marked protection of renal parenchyma was observed. Renal corpuscles looked normal. Most

tubules showed intact epithelium and no casts. Some tubules still showed dilated lumina and eosinophilic deposits.

3.6.2.2. Immunohistochemical assessment of caspase-3 in kidney tissue

Immunostaining of caspase-3 expression in rats' renal tissue showed a negative reaction in G1: C, G2: Vehicle, G3: Crude GA, and G4: GANPs while positive immunostaining was observed in capillaries of glomeruli and those between the tubules and some tubule cells in G5 (receiving BB). On the other hand, tubules with necrotic cells showed a negative reaction. In G6 (GA+BB) and G7 (GA-NPs+BB) showed a decrease in immune expression of caspase-3 immunoreaction was observed in the tubules with superior effect in the group treated with GA-NPs+BB formulation, (Fig. 6).

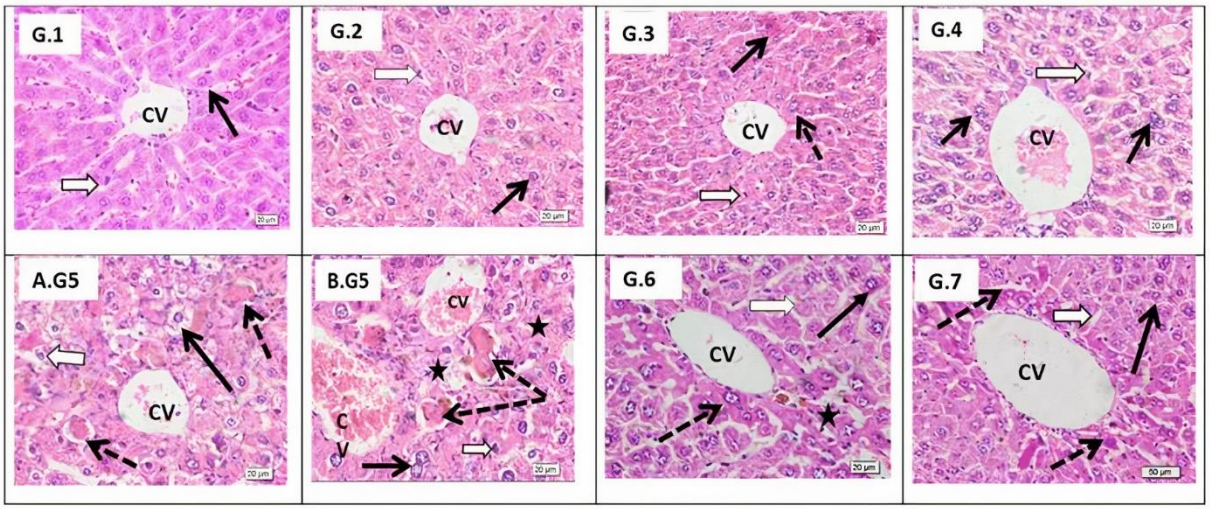

G1 (control): Showing normal central vein (CV) region surrounded by scanty connective tissue. Hepatocyte cell cords showed normal rounded vesicular nuclei (black arrow). Blood sinusoids separating them are of normal appearance and lined with flat endothelial cells (white arrows); G2 (NPs): No changes were observed in CV region. Hepatocytes looked normal and more organized compared to control and showed vesicular active nuclei (black arrow). Blood sinusoids (white arrow) also looked similar to control; G3 (GA): No apparent changes in either hepatocytes or sinusoids were observed except of few cells that showed slightly dense cytoplasm (black arrow) or large nuclei (dotted arrows); G4 (GA-NPs): Showing hepatocytes with more acidophilic cytoplasm with larger vesicular active nuclei, some are binucleated (black arrows). Blood sinusoids were of normal appearance (white arrow); G5 (BB group): Showing A. marked unstained cytoplasm (vacuolation) of hepatocytes (black arrow). Others looked deformed and separated from nearby cells with glassy cytoplasm and peripheral basophilic nuclear debris (dotted arrows) and B. marked central vein dilatation and congestion with disorganization of normal hepatocytes cell cords, Hepatocytes with large nuclei (karyomegaly) or small deformed nuclei could be seen (Black arrow), cell necrosis (stars) and hepatocyte degeneration and clumping (dotted arrows). Hepatic sinusoids showed prominent Kupffer cells (white arrow); G6 (GA+BB): Absence of the marked degenerative changes seen in G5, except of few hepatocytes that showed dark cytoplasm and large nuclei (dotted arrows). Other hepatocytes were of normal structure (black arrow) and the intervening sinusoids also looked normal (white arrow); G7 (GA-NPs+BB): More preservation of normal hepatocytes architecture (black arrows) and sinusoids (white arrow) were observed except of few cells that still showed dark cytoplasm but active vesicular nuclei (dotted arrows).

Fig. 3: Sections from rat's liver from central vein (CV) region stained by H&E

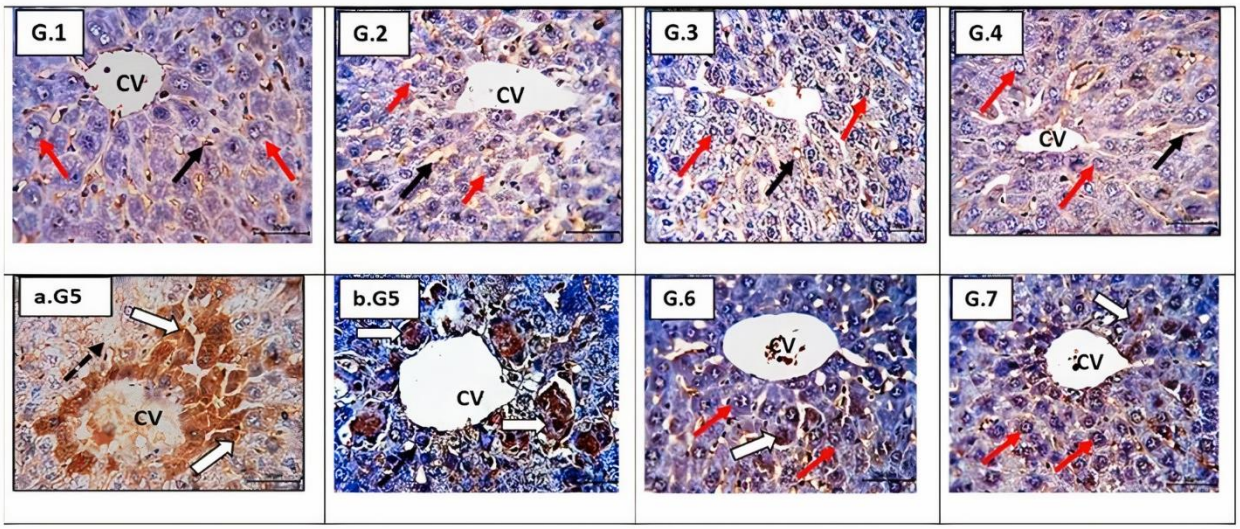

G1 (NC) and G2 (Vehicle) showed negative immuno-expression of caspase-3 apoptotic marker I hepatocyte cytoplasm which showed active rounded vesicular nuclei (red arrows), mild expression I sinusoidal walls (black arrows); G3 (crude gum): Showed mild expression of caspase-3 in sinusoidal endothelial walls cells (black arrows) and negative in hepatocytes cytoplasm which showed rounded one or 3 active vesicular nuclei (red arrows); G4: Normal receiving Nano gum with least expression I groups receiving gum and its nano formulation; G5 a-d (BB group): Showed positive immuno-staining of caspase-3 in degenerated (apoptotic) hepatocytes (White arrows). Notice in the last 2 samples (c-d) apoptotic cells showed separation from nearby cells. Notice also necrotic regions without cell outlines or apparent nuclei (dotted black arrows); G6 (GA+BB): Showed decreased cells expressing positive immunoreaction, only few cells around the central vein could be seen (white arrow). Other cells showed normal active rounded vesicular nuclei (red arrows); G7 (GA-NPs+BB): Showed the least immuno-positively for casapse3, very few positive cells could be seen (white arrow). Notice the active large nuclei (red arrows)

Fig. 4: Sections from the central vein region (CV) of rat liver immuno-stained for caspase-3 and photographed at x400 bar=50µm

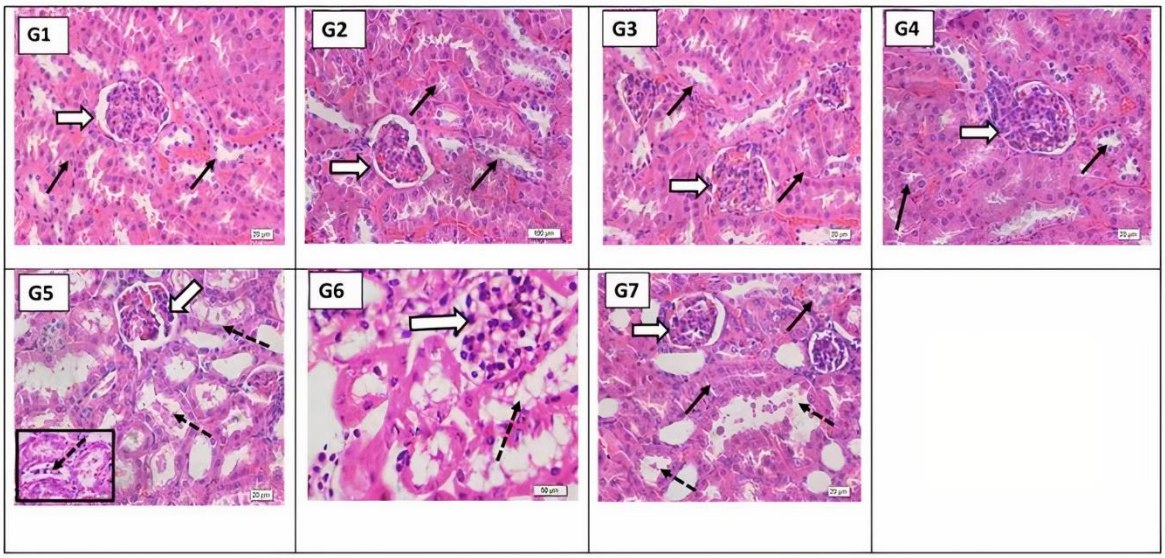

G1 (control): Revealed cortical tissue with normal renal corpuscle and its glomerular capillaries (white arrow). Renal tubules (black arrows) showed normal features with intact cuboidal epithelium and narrow lumina; G2 (NPs): Showed normal architecture with no apparent histological alteration in either renal corpuscle (white arrow) or tubules (Black arrows); G3 (GA): Showing no alteration in renal histological features, renal corpuscle (white arrow) and lining epithelium looked healthier than control (black arrows); G4 (GA-NPs): Showing no histological alteration in renal corpuscles with healthier appearance (large cuboidal cells with active vesicular nuclei) of the tubules lining epithelium (black arrows); G5 (BB group): Showing disorganization of renal corpuscles (white arrow) with glomerular capillaries sclerosis (degeneration/fibrosis). Most renal tubules appeared dilated with degenerated or low-height lining epithelium (dotted arrow). Casts (protein or degenerated cells) could be seen within the dilated lumina (black arrows); G6 (GA+BB): Showed moderate protection of renal corpuscles (white arrow) and tubules (black arrow). Mild protection of tubules that still revealed dilation and luminal deposits (black dotted arrow); G7 (GA-NPs+BB): Showing marked protection of renal parenchyma. Renal corpuscles looked normal (white arrow). Most tubules showed intact epithelium and no casts (black arrows). Some tubules still showed dilated lumina and deposit (dotted arrows).

Fig. 5: Sections from rat's kidney stained by H&E and photographed at x400 bar=20 µm

BB is widely known for being bio-transformed in the liver by cytochrome P450 enzymes into extremely hepatotoxic compounds. The results of this research revealed marked histological damage in liver parenchyma of BB groups in the form of hepatocytes cell cord disorganization due to severe necrotic changes and cell apoptosis. Biochemical analysis showed that serum values of hepatic functional markers (ALT, AST, ALP, and TB) were significantly elevated, while total proteins and albumin were significantly declined in BB-treated groups (BB+GA and BB+GA-NPs groups) versus control.

BB led to functional and morphological changes in hepatocytes cell membranes as revealed by the elevation of liver enzyme activities (Hamed et al., 2013). In the BB group, AST level was markedly elevated than ALT; this might be caused by the increased release of mitochondrial AST and diminished AST clearance due to massive hepatic destruction (Saad et al., 2015). Increased total bilirubin might be due to hemolysis of red blood cells caused by accumulation in blood and the inability of the damaged liver to metabolize free bilirubin (Yavuz et al., 2005). A decline in sera levels of total protein and albumin might be caused by impaired in their formation by the liver, due to hepatic inflammation and oxidative stress, along with elevated protein destruction and loss by the kidney (Yonis and Hassan, 2020).

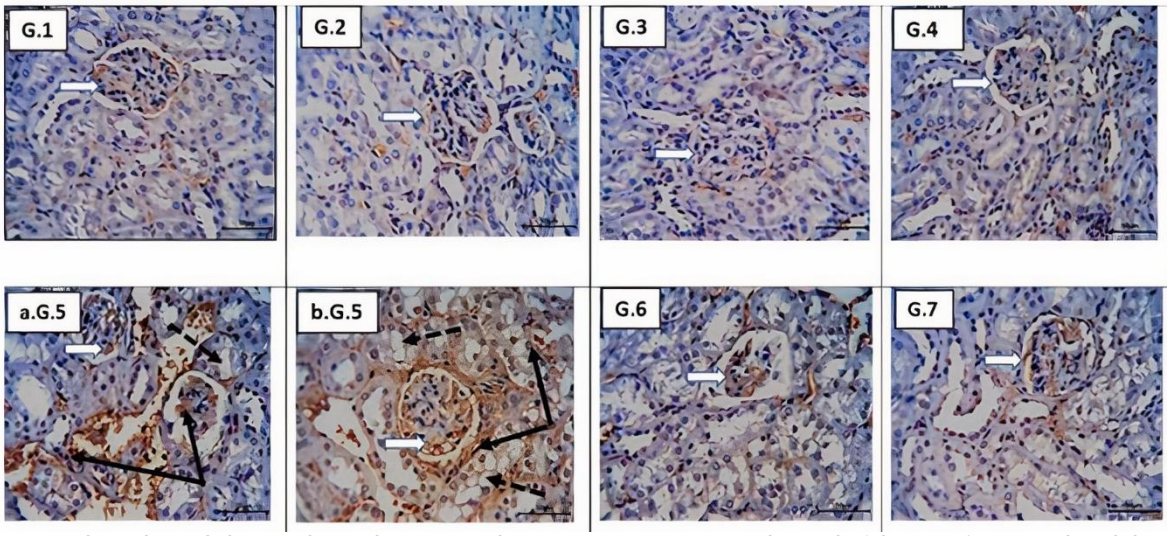

G1: Normal control, G2: Vehicle, G3: crude GA and G4: GA NPs with negative immunoreactions in renal corpuscles (white arrows) or surrounding tubules; G5: BB group showing positive immunoreaction in capillary of glomeruli and between tubules (black arrows) while necrotic tubules showed negative reactions (dotted arrows); G6: BB+GAandG7: BB+GANPs showed a decrease in caspase -3 immunoreaction especially G7 receiving GANPs.

Fig. 6: Sections from rat's kidney immuno-stained for caspase-3 and photographed at x400 bar=50µm

The sera levels of previously reported parameters were improved in rats co-administrated GA and NPs-GA with BB but levels didn't reach the control level. These results were in accordance with histopathological examination results which showed protection against necrotic changes of hepatocytes observed after BB administration. This effect could be attributed to the antioxidant activity of GA that protects against damage to hepatocytes cell membranes and functional integrity with subsequent protection against cellular leakage of enzymes to the circulation. GA was reported to protect mice from acetaminophen-induced liver damage as proven by a significant decline in serum AST, ALT, and hepatic lipid peroxides (Moretti and Marchioni, 2007). Al-Kenanny et al. (2012) reported a decline in AST and ALT in mice treated with GA and gentamycin. Ayaz et al. (2017) reported a marked decline in AST, ALP, ALT, and TB together with an increase in the albumin and TP to about normal in rats with hepatic damage caused by trichloro acetate and pretreated with GA referring to hepato-protective action. Meanwhile, in this research, liver homogenate TAC was significantly decreased in BB-treated groups. Co-administration of GA or GA-NPs increased TAC homogenate levels but it was still significantly lower than normal. It is commonly known that BB oxide depletes glutathione; thus, a reduction in overall cellular redox equilibrium will raise ROS levels. Furthermore, BB phenols, which are metabolites of BB, oxidase to hydroquinone, which also formed ROS. BB intragastric intubation at 10 mmol/kg for 19 hours led to significant changes in antioxidant mechanisms and drug-metabolizing enzymes in the liver (Wang et al., 2007; Gopi and Setty, 2010).

Regarding the kidney studied herein, impairment in renal functions in BB-treated groups was noticed as evidenced by an elevation of serum values of urea, creatinine, and uric acid and a decrease in serum total proteins and albumin. In the kidney, BB metabolites such as 2, 3-epoxy BB, and 2-bromohydroquinone were oxidized to 2-bromoquinone that resulted in the formations of mono and di-substituted metabolites when glutathione combined with them (El-Sharaky et al., 2009; Vedi et al., 2013). This leads to glutathione depletion and nephrotoxicity. Low levels of serum protein in BB-treated groups observed in this study could be due to remarkable protein loss (proteinuria) due to glomeruli and tubules injuries caused by BB nephrotoxicity (Khan et al., 2010; Hamed et al., 2013). Histological disorganization of kidney parenchyma including both necrotic and apoptotic changes in renal corpuscles and tubules induced by BB was much similar to what was previously reported by Hamed et al. (2013) who reported that this damage led to a decline in glomerular filtration rate and decreased renal clearance of creatinine, urea, and uric acid and elevated serum values of these substances.

The present results reveal that GA and its NPs administration for 10 days caused partial improvement in histological and biochemical aspects of BB kidney toxicity. Ali et al. (2003) reported that GA administration (2 mL/kg of a 10% w/v aqueous suspension, orally for ten days) led to a modest partial amelioration of histological changes on acute renal failure caused by gentamicin nephrotoxicity in rats. Saad et al. (2018) reported that GA administration to Adriamycin (50 mg/kg/day, intraperitoneally) feeding rats led to a significant dramatic decline in serum urea, creatinine, blood urea nitrogen, and uric acid to about normal ranges versus Adriamycin treated group. The basis of this protection may be due to GA antioxidant, anti-apoptosis effect. Gum Arabia is a fiber-rich, water-soluble polysaccharide that resists digestion by gut enzymes. GA declines plasma levels of creatinine and urea by binding in the gut to eliminate creatinine and urea from the blood, thus acting as ‘‘enterosorbents’’ and decreasing their circulating values (Nasir, 2013).

Also, in this study kidney tissue homogenate, TAC was significantly decreased in BB-treated groups while partially elevated in GA and GA-NPs co-administrated groups. The observed partial improvement in kidney function parameters and partial elevation of TAC in renal homogenate gives support that GA mops up free radicals generated by BB and offered partial healthy condition for kidney parenchyma, suggesting its action as a renal protective agent.

In the present study, in addition to histological alteration in the liver and kidney observed by routine H&E stain and proved degenerative necrotic and apoptotic changes in both organs, immunohistochemistry revealed that expression of caspase-3 enzyme in liver and kidney tissues was significantly increased in BB-treated groups indicated apoptosis effect of BB (Akkara and Sabina, 2020). Caspase-3 expressions were decreased markedly in GA-treated groups, especially in BB-NPs-treated groups suggesting the anti-apoptosis effect of GA and its nano-formulation. Caspase-3 is a member of the Caspase enzyme family that exerts a central role in the mediation of apoptosis. Apoptosis is a programmed cell death not associated with inflammation and which was well known to be linked to activating initiator caspases (Wen et al., 2020). Liver intoxication usually showed apoptotic changes prior to cell necrosis which could be proved via immunohistochemical staining for Caspase-3 expression. Pro-apoptotic factors were reported to be involved in nephrotoxicity induced by BB (Akkara and Sabina, 2020).

4. Conclusions

From all previous data, it can be concluded that the aqueous extract of GA and its NPs offer significant protection versus BB-induced hepatic and renal injury in rats. Furthermore, the results of this research support the antioxidant, and antiapoptotic properties of GA and its NPs on the liver and kidney functions and structures. Oral admiration of GA and its NPs for 10 days decreased hepatic and renal homogenate levels of total antioxidant capacity and

decreased renal and hepatic expression of caspase-3. Meanwhile, further pharmacological data supporting the action of GA and its NPs versus BB-induced hepatic and renal damages is needed to explore the molecular mechanisms of its action and clinical applications.

Acknowledgment

This author thanks Northern Border University for funding this research. Acknowledgment also was offered to the Nanotechnology unit, Assuit university, and Prof. Soad Shaker; histopathologist KAU, and Assuit University's faculties of medicine for formulation and characterization of nanoparticles besides reviewing the manuscript.

Compliance with ethical standards

Ethics approval

This study was conducted in accordance with ARRIVE Guideline f of Animal and approved by the Ethics Committee of King Abdelaziz University (KAU) (Approval#300-19).

Conflict of interest

The author(s) declared no potential conflicts of interest with respect to the research, authorship, and/or publication of this article.

References

Akkara PJ and Sabina EP (2020). Pre-treatment with beta carotene gives protection against nephrotoxicity induced by bromobenzene via modulation of antioxidant system, pro-inflammatory cytokines and pro-apoptotic factors. Applied Biochemistry and Biotechnology, 190(2): 616-633. https://doi.org/10.1007/s12010-019-03111-0 **PMid:31407161**

Ali BH, Al-Qarawi AA, Haroun EM, and Mousa HM (2003). The effect of treatment with gum arabic on gentamicin nephrotoxicity in rats: A preliminary study. Renal Failure, 25(1): 15-20. https://doi.org/10.1081/JDI-120017439 **PMid:12617329**

Ali BH, Ziada A, Al Husseni I, Beegam S, and Nemmar A (2011). Motor and behavioral changes in rats with adenine-induced chronic renal failure: Influence of acacia gum treatment. Experimental Biology and Medicine, 236(1): 107-112. https://doi.org/10.1258/ebm.2010.010163 **PMid:21239740**

Al-Kenanny ER, Al-Hayaly LK, and Al-Badrany AG (2012). Protective effect of Arabic gum on liver injury experimentally induced by gentamycin in mice. Kufa Journal for Veterinary Medical Sciences, 3(1): 174-189.

Ayaz NO, Ramadan KS, Farid HE, and Alnahdi HS (2017). Protective role and antioxidant activity of Arabic gum against trichloroacetate-induced toxicity in liver of male rats. Indian Journal of Animal Research, 51(2): 303-309. https://doi.org/10.18805/ijar.10976

Bashir M and Haripriya S (2016). Assessment of physical and structural characteristics of almond gum. International Journal of Biological Macromolecules, 93: 476-482. https://doi.org/10.1016/j.ijbiomac.2016.09.009 **PMid:27608543**

Calame W, Weseler AR, Viebke C, Flynn C, and Siemensma AD (2008). Gum arabic establishes prebiotic functionality in healthy human volunteers in a dose-dependent manner. British Journal of Nutrition, 100(6): 1269-1275. https://doi.org/10.1017/S0007114508981447 **PMid:18466655**

El-Sharaky AS, Newairy AA, Kamel MA, and Eweda SM (2009). Protective effect of ginger extract against bromobenzene-induced hepatotoxicity in male rats. Food and Chemical Toxicology, 47(7): 1584-1590. https://doi.org/10.1016/j.fct.2009.04.005 **PMid:19371770**

Emerich DF and Thanos CG (2003). Nanotechnology and medicine. Expert Opinion on Biological Therapy, 3(4): 655-663. https://doi.org/10.1517/14712598.3.4.655 **PMid:12831370**

Gopi S and Setty OH (2010). Beneficial effect of the administration of Hemidesmus indicus against bromobenzene induced oxidative stress in rat liver mitochondria. Journal of Ethnopharmacology, 127(1): 200-203. https://doi.org/10.1016/j.jep.2009.09.043 **PMid:19799985**

Hamed MA, El-Rigal NS, and Ali SA (2013). Effects of black seed oil on resolution of hepato-renal toxicity induced bybromobenzene in rats. European Review for Medical and Pharmacological Sciences, 17(5): 569-581.

Isobe N, Sagawa N, Ono Y, Fujisawa S, Kimura S, Kinoshita K, and Deguchi S (2020). Primary structure of gum arabic and its dynamics at oil/water interface. Carbohydrate Polymers, 249: 116843. https://doi.org/10.1016/j.carbpol.2020.116843 **PMid:32933685**

Khan RA, Khan MR, Sahreen S, and Bokhari J (2010). Prevention of CCl4-induced nephrotoxicity with Sonchus asper in rat. Food and Chemical Toxicology, 48(8-9): 2469-2476. https://doi.org/10.1016/j.fct.2010.06.016 **PMid:20550952**

Laurent S, Saei AA, Behzadi S, Panahifar A, and Mahmoudi M (2014). Superparamagnetic iron oxide nanoparticles for delivery of therapeutic agents: Opportunities and challenges. Expert Opinion on Drug Delivery, 11(9): 1449-1470. https://doi.org/10.1517/17425247.2014.924501 **PMid:24870351**

McNeil SE (2005). Nanotechnology for the biologist. Journal of Leukocyte Biology, 78(3): 585-594. https://doi.org/10.1189/jlb.0205074 **PMid:15923216**

Moretti M and Marchioni CF (2007). An overview of erdosteine antioxidant activity in experimental research. Pharmacological Research, 55(4): 249-254. https://doi.org/10.1016/j.phrs.2006.12.006 **PMid:17267240**

Nasir O (2013). Renal and extra renal effects of gum arabic (Acacia senegal)-What can be learned from animal experiments? Kidney and Blood Pressure Research, 37(4-5): 269-279. https://doi.org/10.1159/000350152 **PMid:24022265**

Nasir O, Wang K, Föller M, Bhandaru M, Sandulache D, Artunc F, and Lang F (2010). Downregulation of angiogenin transcript levels and inhibition of colonic carcinoma by gum arabic (Acacia senegal). Nutrition and Cancer, 62(6): 802-810. https://doi.org/10.1080/01635581003605920 **PMid:20661830**

Pannala VR, Estes SK, Rahim M, Trenary I, O'Brien TP, Shiota C, and Wallqvist A (2020). Mechanism-based identification of plasma metabolites associated with liver toxicity. Toxicology, 441: 152493. https://doi.org/10.1016/j.tox.2020.152493 **PMid:32479839**

Park EY, Murakami H, and Matsumura Y (2005). Effects of the addition of amino acids and peptides on lipid oxidation in a powdery model system. Journal of Agricultural and Food Chemistry, 53(21): 8334-8341. https://doi.org/10.1021/jf058063u **PMid:16218685**

Rao K, Aziz S, Roome T, Razzak A, Sikandar B, Jamali KS, and Shah MR (2018). Gum acacia stabilized silver nanoparticles based nano-cargo for enhanced anti-arthritic potentials of

hesperidin in adjuvant induced arthritic rats. Artificial Cells, Nanomedicine, and Biotechnology, 46(sup1): 597-607. https://doi.org/10.1080/21691401.2018.1431653 **PMid:29381085**

Saad EA, El-Gayar HA, EL-Demerdash RS, and Radwan KH (2018). Hepato-toxic risk of gum arabic during adenine-induced renal toxicity prevention. Journal of Applied Pharmaceutical Science, 8(12): 104-111. https://doi.org/10.7324/JAPS.2018.81212

Saad EA, Toson ESA, and Ahmed GM (2015). Cloveor green tea administration antagonizeskhat hepatotoxicity in rats. International Journal of Pharmacy and Pharmaceutical Sciences, 7(6): 72-76.

Vedi M, Kalaiselvan S, Rasool M, and Sabina EP (2013). Protective effects of blue green algae Spirulina fusiformis against galactosamine-induced hepatotoxicity in mice. Asian Journal of Pharmaceutical and Clinical Research, 6(3): 150-154.

Wang CY, Ma FL, Liu JT, Tian JW, and Fu FH (2007). Protective effect of salvianic acid an on acute liver injury induced by carbon tetrachloride in rats. Biological and Pharmaceutical Bulletin, 30(1): 44-47. https://doi.org/10.1248/bpb.30.44 **PMid:17202657**

Wen S, Wang ZH, Zhang CX, Yang Y, and Fan QL (2020). Caspase-3 promotes diabetic kidney disease through gasdermin E-mediated progression to secondary necrosis during apoptosis. Diabetes, Metabolic Syndrome and Obesity: Targets and Therapy, 13: 313-323. https://doi.org/10.2147/DMSO.S242136 **PMid:32104028 PMCid:PMC7020918**

WHO (1974). Evaluations of some pesticide residues in food. World Health Organization, Geneva, Switzerland.

Williams PA and Phillips GO (2021). Gum arabic. In: Phillips GO and Williams PA (Eds.), Handbook of hydrocolloids: 627-652. 3rd Edition, Woodhead Publishing, Sawston, UK. https://doi.org/10.1016/B978-0-12-820104-6.00022-X

Xie J, Liu G, Eden HS, Ai H, and Chen X (2011). Surface-engineered magnetic nanoparticle platforms for cancer imaging and therapy. Accounts of Chemical Research, 44(10): 883-892. https://doi.org/10.1021/ar200044b **PMid:21548618 PMCid:PMC3166427**

Yavuz A, Tetta C, Ersoy FF, D'intini V, Ratanarat R, De Cal M, and Ronco C (2005). Reviews: Uremic toxins: A new focus on an old subject. Seminars in Dialysis, 18(3): 203-211. https://doi.org/10.1111/j.1525-139X.2005.18313.x **PMid:15934967**

Yonis WK and Hassan AH (2020). Antioxidant activity of spirulina powder in male rate with adenine–induced chronic renal failure. Medico-Legal Update, 20(4): 1725-1729. https://doi.org/10.37506/mlu.v20i4.2082

Zhang L, Yu F, Cole AJ, Chertok B, David AE, Wang J, and Yang VC (2009). Gum arabic-coated magnetic nanoparticles for potential application in simultaneous magnetic targeting and tumor imaging. The AAPS Journal, 11(4): 693-699. https://doi.org/10.1208/s12248-009-9151-y **PMid:19842043 PMCid:PMC2782085**